Heterogenous columnar-grained high-entropy alloys produce exceptional resistance to intermediate-temperature intergranular embrittlement

B.X. Cao [a], H.J. Kong [a], L. Fan [b], J.H. Luan[a], Z.B. Jiao[b], J.J. Kai [c,d], T. Yang [a,e,*] , C.T. Liu[a,e,*]

[a] *Department of Materials Science and Engineering, City University of Hong Kong, Hong Kong, China*
[b] *Department of Mechanical Engineering, The Hong Kong Polytechnic University, Hong Kong, China*
[c] *Department of Mechanical Engineering, City University of Hong Kong, Hong Kong, China*
[d] *Center for Advanced Nuclear Safety and Sustainable Development, City University of Hong Kong, Hong Kong, China*
[e] *Hong Kong Institute for Advanced Study, City University of Hong Kong, Hong Kong, China*

Abstract

High-entropy alloys (HEAs) strengthened by coherent nanoparticles show great potentials for elevatedtemperature structural applications, which however, generally suffer from a severe intergranular embrittlement when tested at intermediate temperatures. In this study, we demonstrated a novel "heterogenous columnar-grained" (HCG) approach that can effectively overcome this thorny problem. Different from the equiaxed counterpart which shows extreme brittleness along grain boundaries at 800°C, the newly de- veloped HCG-HEA exhibits an exceptionally high resistance to intergranular fractures originating from the unique grain-boundary characters and distributions. The presence of heterogenous columnar grain structure drastically suppresses the crack nucleation and propagation along with boundaries, resulting in an unusually large tensile ductility of ~18.4 % combined with a high yield strength of ~652 MPa at 800°C. This finding provides a new insight into the innovative design of

high-temperature materials with extraordinary mechanical properties.

The face-centered-cubic (FCC) high-entropy alloys (HEAs) strengthened by high-density coherent L12-type nanoparticles have garnered significant interest among the materials community due to their many unique structural features and mechanical properties[1-7]. The intrinsically ductile natures of both the multi- component FCC matrix and L12 precipitate, together with the coherent FCC/L12 interfaces, make these nanoparticles-strengthened HEAs showing excellent strength-ductility combinations at both ambient and cryogenic temperatures[8]. For example, when de- formed at $-196\,°C$, a combined increase rather than decrease in tensile ductility up to 40-50% can be achieved even under a high yield strength around 1 GPa[9,10]. What is more commendable is their great potential for high-temperature structural applications[4,11,12]. As compared with the single-FCC HEAs, the pres- ence of dense precipitation produces strong barriers to dislocation motion, enabling them with outstanding resistance against soft- ening and creep at elevated temperatures[11]. More intriguingly alloying of multiple principal elements in the HEA systems gives rise to increased activation energies for elemental diffusion, which consequently results in an enhanced coarsening resistance of the $L1_2$ precipitate when compared with many other conventional Ni-based superalloys[8,13,14]. For example, Pandey et. al.[13] systematically investigated the

temporal evolutions of $L1_2$ precipitates in the Ni-37.6Co-9.9Al-4.9Mo-5.9Cr-2.8Ta-3.5Ti (at. %) HEA. An excellent coarsening resistance was achieved, resulting from a high activation energy (determined to be about 360kJ/mol) for coarsening and the associated sluggish diffusion effect. Similar results have also been identified in our recent studies in the Ni-30Co-13Fe-15Cr-6Al-6Ti-0.1B (at.%) HEA[14]. The high-volume fraction of coherent $L1_2$-type precipitates coupled with their excellent thermal stability render this kind of nanoparticles-strengthened HEAs highly attractive for elevated-temperature applications with potentially superior mechanical properties.

Unfortunately, most exiting alloys in polycrystalline forms usually suffer from a serious intergranular embrittlement at the intermediate temperatures, in particular at the temperature of 800°C[15-17]. The sudden and rapid fractures along grain boundaries upon tensile deformation set one of the most severe limits on their practical applications. Similar embrittling behaviors have also been frequently observed in many commercial Ni-based superalloys, such as the U720Li and GH4033, etc[18-20]. The conventional view generally links such a property degradation to the undesired precipitation of detrimental phases at grain boundaries. As a result, considerable efforts have been devoted to removing the intergranular brittle phases by tuning the chemical compositions or processing conditions[14-16]. However, such approach in practice appears not to be the key determinant to solve this embrittlement problem from the root. For instance, many $L1_2$-strengthened high-strength alloys, even without brittle phases along grain boundaries, still exhibit extreme brittleness along grain boundaries when subjected to tensile deformation at 800°C[17,18,20]. One notable example was reported in the GH4033

alloy strengthened by an uniform precipitation of L1$_2$-type nanoparticles[20]. Although a decent yield strength of 467MPa can be achieved, the fracture was completely brittle dominated by intergranular cracks. It is important to note that grain-boundary character is known to be an im- portant microstructural feature that strongly affects the mechanical and physicochemical properties of polycrystalline materials. Control and design of grain boundaries have been extensively studied in various materials to improve their resistance to oxidation, corrosion, and fatigue[21-23]. We found that, however, the equiaxed grain structure was most commonly adopted as a "standard" structure in previous studies for the development of L1$_2$-strengthened HEAs, as well as the wrought superalloys. This prompts us must seriously consider: can we alleviate the serious intergranular brit- tleness through manipulating the grain-boundary features?

Along with this line of thinking, in the present work, we attempt to explore the feasibility of eliminating the intermediate-temperature embrittlement in the high-strength L1$_2$-strengthened HEAs by tailoring grain-boundary characters and distributions. Departing from the previous design that was mainly focused on achieving the equiaxed grain structures, here we deliberately in- troduce the heterogenous columnar-grained structure by a simple thermomechanical treatment process for intergranular toughening. In this study, the microstructures, tensile behaviors, as well as underlying plastic deformation and fracture mechanisms were carefully investigated.

To start with, the multicomponent Ni-30Co-13Fe-15Cr-6Al-6Ti-0.1B (at.%) HEA with an excellent thermal stability and dense pre- cipitation of L1$_2$-type nanoparticles, was selected as a model alloy in the present study[14]. This alloy was prepared by arc

melting under a high-purity argon atmosphere. All ingots were repeatedly melted for at least five times to promote the compositional ho-mogeneity and then cast into a copper mold with a dimension of $50 \times 12 \times 5mm^3$. As-cast slats were subsequently homogenized at ~1150°C for 2h and then cold rolled to around 1.7mm along the longitudinal direction. Afterward, we architected the heterogenous columnar-grained structure (denoted as HCG-HEA hereafter) by annealing the cold-rolled sheets (~65 × $15 \times 1.7mm^3$) at ~1150°C for 20 sec (insert and take out the samples using a tweezer), followed by subsequent aging at 1000°C for 4h and 800°C for 16h, respectively. The equiaxed grained counterpart (denoted as EG-HEA hereafter) was prepared by annealing the cold-rolled sheets at ~1150°C for 2.5min combined with the same duplex aging treatment. To avoid possible cracks caused by water quenching, all heat treatments adopted here were finished by air cooling to room temperature. Microstructural characterizations were carried out using a field-emission scanning electron microscope (FE- SEM, FEI, Scios) and transmission electron microscope (TEM, JEOL-2100F). Electron backscattered diffraction (EBSD) characterizations were performed using an Oxford Instrument's detector. Compositional analyses were conducted using a TEM energy-dispersive X-ray spectroscopy (TEM-EDS) and three-dimensional atom probe tomography (3D-APT). Detailed procedures for specimen preparations were described in our previous study[14,24]. Flat dog-bone-shaped specimens with a gauge length of 12.5mm and a crosssection dimension of 3.2 × $1.5mm^2$ were fabricated by electrodischarge machining for tensile tests. Each side of the specimens was carefully polished using 2500-grit SiC papers. The uniaxial tensile

tests were performed at 800°C in air condition with a constant strain rate of 1×10^{-3} s^{-1}. Three specimens were tested to confirm the reproducibility, and representative curves were displayed.

The microstructures and grain-boundary characters were carefully investigated by multiscale microstructural analyses, as shown in Fig. 1 (a-f). The EG-HEA exhibited a fully equiaxed microstructure with an average grain size of 42μm (see Fig. 1(a)). The uniform precipitation of ductile L1$_2$-type nanoparticles with a bimodal size distribution can be clearly evidenced (inset in Fig. 1(b)). Distinctly different from the EG-HEA, the newly developed HCG-HEA exhibits a mixed grain structure consisting of fine equiaxed-grained region separated by the coarser columnar-grained region (see Fig. 1(c)). High-density L1$_2$ particles can be clearly observed without precipitation of other intermetallic compounds at the grain boundaries (inset in Fig. 1(c)). Chemical compositions of the individual phases were carefully determined by the TEM-EDS and 3D-APT. Fig.. 1(d) shows the typical atom maps collected from the HCG-HEA. Evidently, the Ni, Ti and Al atoms strongly partition into the L1$_2$ nanoparticles. The mole fractions of L1$_2$ precipitates of these two HEAs were estimated to be approximately 38% via the lever rule. Furthermore, representative EBSD images of the alloys were presented in Fig. 1(e), and the grain-boundary characters and distributions were summarized in Fig. 1(f) accordingly. It can be clearly observed that the EG-HEA was dominated by high-angle random grain boundaries (HARGBs), where there is a high de- gree of connectivity between them. Some amounts of coincidence site lattice grain boundaries (CSLGBs) can be identified, which were mainly distributed in the

grain interior. In contrast, the HCG- HEA exhibits increased fractions of low-angle grain boundaries (LAGBs, $3°<\theta<15°$). Most notably, by incorporating these coarse columnar-grained regions, the connectivity of HARGBs was sub- stantially disrupted. As shown in Fig. 1(e), the maximum HARGB cluster length of the EG-HEA and HCG-HEA can be estimated to be about 6368 and 97μm, respectively. Previous studies revealed that the HARGBs were highly vulnerable to crack initiating and propagating, especially when they connect with each other to form a network[25-27]. Further detailed analyses revealed that the remarkable changes in the grain-boundary structures play a crucial role in determining the plastic deformability of these alloys.

Fig. 2(a) shows the representative tensile curves of the Ni-30Co-13Fe-15Cr-6Al-6Ti-0.1B (at.%) HEAs with various grain structures tested at 800°C in air condition. We surprisingly found a distinct brittle-to-ductile transition in these high-strength alloys, showing a significant increase of tensile ductility at a comparable level of yield strength. Owing to the high-volume fraction of L1$_2$-type pre- cipitates, the EG-HEA alloy showed an appreciable yield strength of ~642 ± 7 MPa at this temperature. Although a relatively uniform distribution of grains and precipitates was achieved, it suffers from extreme brittleness at this temperature, which failures rapidly once after yielding with almost no plastic deformability. The poor tensile ductility (~2.0 ± 0.4 %) can be ascribed to the serve intergranular embrittlement, which was clearly evidenced from the fractured surfaces containing massive cleavage facets and cracks along the grain boundaries, as displayed in Fig. 2(b). Such a serious embrittling behavior has also been widely observed in many other L1$_2$-strengthened HEAs and superalloys with

comparable yield strengths[15,16,18]. In strong contrast, by changing the grain structure from equiaxed grains to heterogenous columnar grains, the intergranular embrittlement can be substantially alleviated. As can be seen in Fig. 2(a), the HCG-HEA exhibit a large tensile ductility of about $18.4 \pm 2.8\%$ and a high yield strength of $\sim 652 \pm 27$ MPa, accompanied by a fully ductile facture mode dominated by numerous fine dimples (see Fig. 2(b)). Moreover, a direct comparison of the tensile yield strength and ductility of the present HCG-HEA with those of many other advanced Ni-based superalloys and multicomponent HEAs[15-20,28] was presented in Fig. 2(c). Clearly, the newly developed HCG-HEA is located at the upper-right corner above the general curve of previous alloys, which indicates a much superior strength-ductility combination at this temperature, making it with considerably enhanced potentials for structural applications at elevated temperatures.

These results successfully demonstrated the feasibility of eliminating the intermediate-temperature embrittlement by manipulation of grain-boundary characters and distributions. We next focus on unveiling the structural origins underlying such an impressive ductilization behavior. Microstructures of the failed speci- mens were carefully analyzed by SEM and EBSD characterizations. Fig. 3(a) shows a secondary electron SEM image of the fractured EG-HEA after tensile tests. There are extensive large cracks (both primary and secondary) observed near the fractured end in an intergranular manner. The EBSD mapping (see Fig. 3(c-f)) further revealed that the local stress was concentrated primarily along the HARGBs (see Fig. 3(e)), which can be attributed to the onset of slip-assisted grain-boundary sliding and the accumulation

of dislocations at the vicinity of them[18,29]. These HARGBs can be identified as preferred sites or paths for crack initiation and propagation in the EG-HEA, where multiple cracks were identified along with them (see Fig. 3(f)). Similar intergranular cracking behaviors under comparable testing conditions have also been found in many other equiaxed Ni-based superalloys[18]. As compared to the LAGBs and CSLGBs, the HARGBs have been reported to more prone to cracking due to their relatively higher energies and activities[25,26,30,31]. As shown in Fig. 1, a higher fraction of HARGBs which connected to each other was observed in the EG- HEA. Once cracks are initiated, they will spread rapidly along these HARGBs and cause the brittle failure. Moreover, it was well demonstrated that this intergranular oxidation takes place preferentially at the HARGBs, which in turn leads to the dynamic environmental embrittlement of grain boundaries[18,22,32,33]. For alloys tested in oxidizing environments at elevated temperatures, the absorbed oxygen will embrittle grain boundaries and promotes the initiation of cracks long with them. Once theses intergranular microcracks are formed, continuous penetration of oxygen at the crack tips accelerates the rapid propagation of them when exposed to increased tensile stress. Although some amounts of CSLGBs were identified in the EG-HEA, they were essentially formed in the grain interior and thus fail to prevent the serious cracking along the HARGBs.

Remarkedly, the intergranular embrittlement was significantly inhibited in the HCG-HEA. As clearly evidenced in Fig. 3(b), only small amounts of circle-like micro-voids with blunted edges were identified on the surfaces, which were separated from each other without long-distance coalescence even when subjected to a large amount of

plastic deformation (around 18% strain). The large tensile ductility that we achieved can be primarily ascribed to the following two aspects. On one hand, the alternately existed largesize columnar grains play an important role in suppressing the brittle fracture along grain boundaries. The beneficial effect of them is to greatly disrupt the connectivity of HARGBs, and thereby block the path of crack propagation. As shown in Fig. 3(b), even if some small micro-voids nucleated at the boundaries of the finegrain region, these voids were effectively stopped by the adjacent large-sized columnar grain because of the difficulty in propagating them within this region. On the other hand, the increased formation of LAGBs, which were reported with relatively high resistance to fracture and oxidation damages, will also contribute to the improved immunity of alloys to early fracture along boundaries[26]. Benefiting from these factors, the fracture mode changes from intergranular fracture to trans-granular fracture, resulting in a substantial increase of tensile ductility in the HCG-HEA. Crack propagation processes in present polycrystalline HEAs with differ- ent grain-boundary microstructures were schematically illustrated Fig. 4. Obviously, reducing HARGBs and their connectivity is the key determinant of eliminating the intergranular embrittlement. It is also worthy to mention that directional-solidification or singlecrystal technique is expected to give the enhanced fracture resistance of these alloys[17,34]; however, these techniques generally requires extremely complicated processes with high costs and long production cycles. By comparison, as we demonstrated above, the heterogenous columnar-grained design with desired grain-boundary configurations can be implemented effectively by a simple and controllable thermomechanical procedure. It

provides a highly cost-effective and time-efficient strategy for developing strong-yet-ductile high-temperature structural materials, which should be of particular interest for those alloys to be used in the intermediate-temperature regime. In addition, in comparison to the EG-HEA alloy, given the excellent immunity to inter- granular degradation, an enhanced creep resistance at intermediate temperatures can be expected in the HCG-HEA, which might be comparable to that of the directional-solidification or single-crystal counterparts. Comparative analysis on their creep properties merits systematic investigations in the future. It is also noteworthy that the performance anisotropy of heterogenous structures should be taken into consideration during the practical service.

In summary, we proposed and demonstrated a novel grain- boundary design approach that can be leveraged to effectively eliminate the intermediate-temperature embrittlement of high- strength HEAs strengthened by high-density $L1_2$-type coherent nanoparticles. On the basis of multiple experimental techniques, the grain structures, mechanical properties, as well as the underlying fracture mechanisms have been carefully investigated.

When tensioned at 800°C in air condition, the specimens with an equiaxed grain structure fractured rapidly along HARGBs with a negligible tensile ductility. In a strong contrast, the heterogenous columnar-grained HEAs exhibited an excellent tensile ductility up to ~18.4 % and a high yield strength of ~652 MPa, accompa- nied by a ductile transgranular fracture mode with numerous fine dimples. Such a pronounced brittle-to-ductile transition achieved here was mainly ascribed to the presence of

large-size columnar grains and also the increased fractions of LAGBs, which drastically reduce the connectivity of HARGBs and consequently suppresses the nucleation and propagation of cracks along with them. These findings will not only advance the mechanistic understanding of the intergranular embrittling behaviors of nanoparticles strengthened alloys but also provide a promising pathway for developing new-type high-temperature structural materials with en- hanced strength-ductility combinations.

Declaration of Competing Interest

The authors declare that they have no known competing finan- cial interests or personal relationships that could have appeared to influence the work reported in this paper.

wrote the manuscript. The authors declare no competing interests.

References

[1]   1. J.Y. He, H. Wang, H.L. Huang, X.D. Xu, M.W. Chen, Y. Wu, X.J. Liu, T.G. Nieh,   K. An, Z.P. Lu, Acta Mater 102 (2016) 187–196.

[2]   2. T. Yang, Y.L. Zhao, Y. Tong, Z.B. Jiao, J. Wei, J.X. Cai, X.D. Han, D. Chen, A. Hu,   J.J. Kai, K. Lu, Y. Liu, C.T. Liu, Science 362 (6417) (2018) 933–937.

[3]   3. Y. Liang, L. Wang, Y. Wen, B. Cheng, Q. Wu, T. Cao, Q. Xiao, Y. Xue, G. Sha, Y. Wang, Nature communications 9 (1) (2018) 1–8.

[4]   4. J. Brechtl, S.Y. Chen, X. Xie, Y. Ren, J.W. Qiao, P.K. Liaw, S.J. Zinkle, Int. J. Plast 115 (2019) 71–92.

[5]   5. C. Slone, E.P. George, M.J. Mills, J. Alloys Compd. 817 (2020) 152777.

[6]   6. Y.L. Zhao, T. Yang, B. Han, J.H. Luan, D. Chen, W. Kai, C.T. Liu, J.J. Kai, Materials Research Letters 7 (4) (2019) 152–158.

[7]   7. L. Guo, J. Gu, X. Gong, S. Ni, M. Song, Science China Materials 63 (2) (2020) 288–299.

[8]   8. T. Yang, Y.L. Zhao, B.X. Cao, J.J. Kai, C.T. Liu, Scr. Mater. 183 (2020) 39–44.

[9]   9. T. Yang, Y.L. Zhao, J.H. Luan, B. Han, J. Wei, J.J. Kai, C.T. Liu, Scr. Mater. 164 (2019) 30–35.

[10]   10. Y. Tong, D. Chen, B. Han, J. Wang, R. Feng, T. Yang, C. Zhao, Y.L. Zhao, W. Guo, Y. Shimizu, C.T. Liu, P.K. Liaw, K. Inoue, Y. Nagai, A. Hu, J.J. Kai, Acta Mater 165 (2019) 228–240.

[11]   11. T.K. Tsao, A.C. Yeh, C.M. Kuo, K. Kakehi, H. Murakami, J.W. Yeh, S.R. Jian, Scien- tific reports 7 (1) (2017) 1–9.

[12]   12. J. Chen, X. Zhou, W. Wang, B. Liu, Y. Lv, W. Yang, D. Xu, Y. Liu, J. Alloys Compd. 760 (2018) 15–30.

[13]   13. P. Pandey, S. Kashyap, D. Palanisamy, A. Sharma, K. Chattopadhyay, Acta Mater 177 (2019) 82–95.

[14]   14. T. Yang, Y.L. Zhao, L. Fan, J. Wei, J.H. Luan, W.H. Liu, C. Wang, Z.B. Jiao, J.J. Kai, C.T. Liu, Acta Mater (2020).

[15]   15. C.M. Kuo, C.W. Tsai, Mater. Chem. Phys. 210 (2018) 103–110.

[16]   16. Y.J. Chang, A.C. Yeh, Mater. Chem. Phys. 210 (2018) 111–119.

[17]   17. S. Haas, A.M. Manzoni, F. Krieg, U. Glatzel, Entropy 21 (2) (2019) 169.

[18]   18. A. Németh, D. Crudden, D. Armstrong, D. Collins, K. Li, A. Wilkinson, C. Grovenor, R. Reed, Acta Mater 126 (2017) 361–371.

[19]   19. A.K. Roy, A. Venkatesh, V. Marthandam, A. Ghosh, J. Mater, Eng. Perform. 17 (4) (2008) 607–611.

[20]   20. J. Ma, W. Li, X. Zhang, H. Kou, J. Shao, P. Geng, Y. Deng, D. Fang, Mater. Sci.   Eng., A 676 (2016) 165–172.

[21]   21. H.W. Liu, Y. Oshida, (1986).

[22]   22. S. Yamaura, Y. Igarashi, S. Tsurekawa, T. Watanabe, in: Properties of Complex Inorganic Solids 2, Springer, 2000, pp. 27–37.

[23]   23. E. West, G. Was, J. Nucl. Mater. 392 (2) (2009) 264–271.

[24]   24. Y.L. Zhao, T. Yang, Y.R. Li, L. Fan, B. Han, Z.B. Jiao, D. Chen, C.T. Liu, J.J. Kai, Acta Mater (2020).

[25]   25. T. Watanabe, Toughening of brittle materials by grain boundary design and control, Mater. Sci. Forum Trans Tech Publ (1993) 295–304.

[26]   26. T. Watanabe, Mater. Sci. Eng., A 176 (1-2) (1994) 39–49.

[27]   27. C.A. Schuh, M. Kumar, W.E. King, Acta Mater 51 (3) (2003) 687–700.

[28]   28. K. Ming, L. Li, Z. Li, X. Bi, J. Wang, Science Advances 5 (12) (2019) eaay0639.

[29]   29. D.A. Woodford, Energy Materials 1 (1) (2006) 59–79.

[30]   30 H. Gleiter, Physica status solidi (b) 45 (1) (1971) 9–38.

[31]   31. T. Watanabe, Mater. Sci. Eng., A 166 (1-2) (1993) 11–28.

[32]   32. K. Fujii, T. Miura, H. Nishioka, K. Fukuya, in: Degradation of grain boundary strength by oxidation in alloy 600, Proceedings of the 15th International Con- ference on Environmental Degradation of Materials in Nuclear Power System- s—Water Reactors, Springer, 2011, pp. 1447–1461.

[33]   33. L. Tan, K. Sridharan, T. Allen, J. Nucl. Mater. 348 (3) (2006) 263–271.

[34]   34. C.T. Liu, B.F. Oliver, J. Mater. Res. 4 (2) (1989) 294–299.

Figure captions

Fig. 1. (a) Schematic illustration of the tensile sample. **(b)** Representative SEM images collected from the EG-HEA with an equiaxed grain structure. **(c)** Representative SEM images of collected from the HCG-HEA with a heterogenous columnar-grained structure. Insets show the high-density $L1_2$ particles without precipitation of other intermetallic compounds at the grain boundaries. **(d)** Representative atom maps collected from the HCG-HEA by using the 3D-APT. **(e)** Representative EBSD inverse pole figure (IPF) and corresponding grain-boundary maps (inset). **(f)** Grain boundary characters and distributions the present HEAs with distinctly different grain structures.

Fig. 2. (a) Engineering tensile curves of the present HEAs with different grain structures tested at 800°C in air. **(b)** SEM fractographs of the EG-HEA and HCG-HEA tested at 800°C in air, respectively. Heterogenous columnar-grained structure enables a distinct brittle-to-ductile transition with exceptional resistance to intergranular embrittlement.Superior mechanical properties of the present HCG-HEA compared to various high-performance wrought Ni-based superalloys and HEAs.

Fig. 3. (a) SEM images showing the serious intergranular cracking of the EG-HEA tested at 800°C in air. **(b)** SEM images showing the excellent crack resistance of the HCG-HEA tested at 800°C in air. **(c)** A close view of magnified SEM image and **(d)** band contrast map collected from the intergranular cracks in **Fig. 3(a). (e)** Corresponding kernel average misorientation (KAM) map and **(f)** inverse pole figure
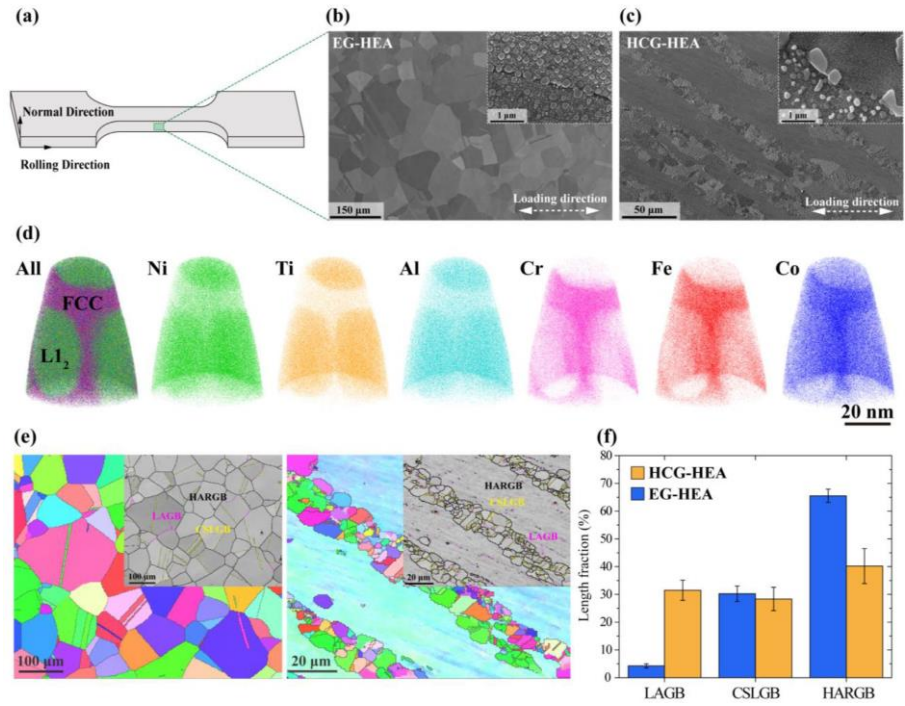
(IPF) map, which show the serious stress concentration localized at the HARGBs and associated crack propagation along them.

Fig. 4. Schematic illustration showing the effect of grain structures on the fracture mechanisms of the present HEAs. Engineering heterogenous columnar-grained structure produces a remarkable ductilization effect by inhibiting the intergranular cracking.
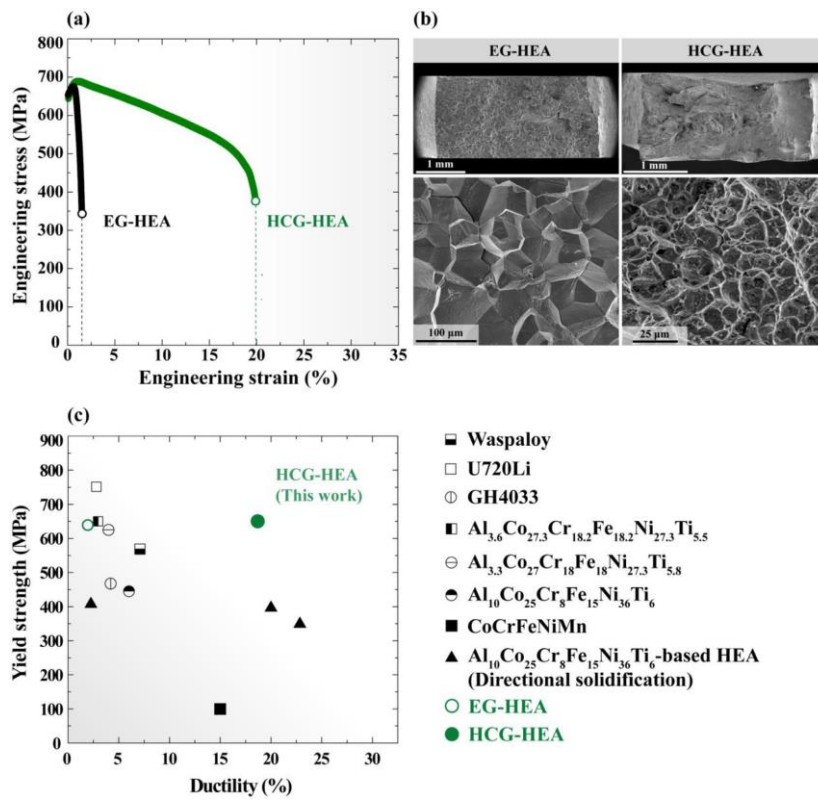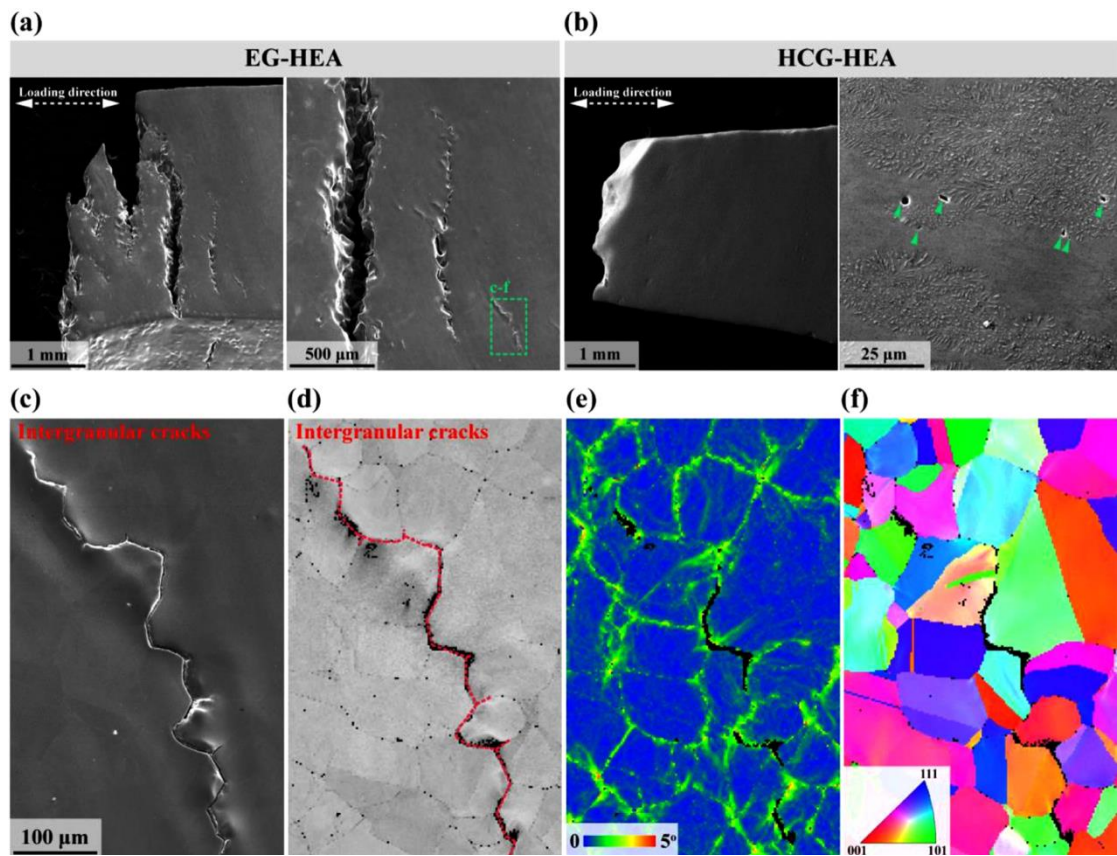
Fig 1

Figure list and legends

Fig 2

Fig 3

(a) EG-HEA — Loading direction — 1 mm — 500 μm — c-f

(b) HCG-HEA — Loading direction — 1 mm — 25 μm

(c) Intergranular cracks — 100 μm

(d) Intergranular cracks

(e) 0 — 5°

(f) 111 — 001 — 101

Fig 4